Electronic Structure of Oxygen in the Defective Nickel Monoxide

Kwang-Soon Lee*†, Hyun-Joo Koo, Kyoung-Hee Ham, and Woon-Sun Ahn

Department of Chemistry, Sung Kyun Kwan University, Suwon 440-746, Korea
†Department of Chemistry, Song Sim University, Puchon 422-743, Korea
Received September 26, 1994

The band structure of nickel monoxide having a cation defect rock salt structure is calculated by means of the tight-binding extended Hückel method. The calculation is also made for the net charge, the DOS, the COOP, the electron density of the constituent atoms, and the O 1s binding energy shift when one of the adjacent nickel atoms is defected. It is found that the band gap near the Γ on the Brillouin zone is about 0.2 eV, and that all of the properties calculated including the electronic structure of the oxygen atom are more effectively affected by the surface defect than the inside one. The core O 1s binding energy shift is calculated by the use of valence potential method and the results are very satisfactory in comparison with the XPS experimental findings.

Introduction

Nickel oxide with the rock salt structure has been known to show antiferromagnetic insulating[1~3] behavior when it has stoichiometric structure. Mattheiss[4,5] attempted to explain the behavior with its band structure by the use of augmented plane wave method, but was not so successful in describing the insulating nature. The insulating magnetic behavior was successfully explained by Oguchi *et al.*[6,7] by the use of band theory based on the local spin density functional method.

The nickel oxide shows, however, a considerable semiconductivity when it is heated in the air. The heating introduces Ni^{2+} vacancies into the NiO structure, and these vacancies cause the oxidation of Ni^{2+} ions around the vacancy to Ni^{3+} ions at the same time. The conduction is explained as a result of the migration of this Ni^{3+} ions as a consequence of electron hopping between the Ni^{2+} and Ni^{3+} ions.[8] The vacancy gives the oxide the catalytic activity in addition.[9~12] It has been known that the defected nickel oxide interact with oxygen molecule to dissociate it, and that the defects play an important role in the catalytic activity.[11,12]

The X-ray photoelectron spectra of the defected nickel oxide show extra O 1s peaks of higher binding energy in addition to the typical O 1s peak of the perfect metal oxide oxygen.[13] The shifted O 1s binding energies are attributed to the presence of Ni^{3+} ions and/or other impurities such as OH^-, CO_3^{2-}, and O_2^- ions around the oxygen atoms.[14] Meanwhile, the temperature programmed thermal desorption spectrum shows also the presence of three oxygen species of different desorption energy. They are attributed to the different coordination number the oxygen atom takes in the oxide.[15] It will be interesting to find out how the band structure changes and what extent the core electron binding energy of oxygen changes upon the defect introduction.

No theoretical works of this kind has been reported for the transition metal oxides with a semiempirical method yet. The band structure, the density of state (DOS), the crystal orbital overlap population (COOP), and the core electron binding energy shift of oxygen atom are calculated in connection with the cation defect in nickel oxide in this work. The calculation is made with the tight binding EH type method, with which Hoffmann[16~19] and Whangbo *et al.*[20,21] initiated the theoretical study of solid state compounds successfully.

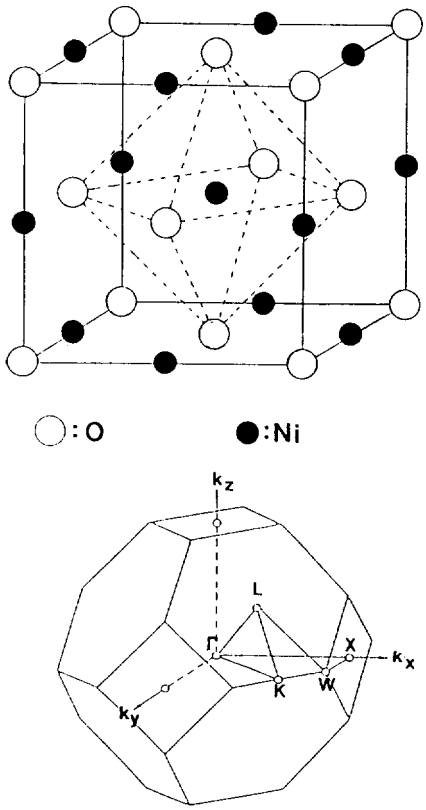

Figure 1. Unit cell of nickel oxide and its corresponding Brillouin zone.

Results

Band structure of NiO. The unit cell of nickel oxide is taken as shown in Figure 1 with corresponding fcc Brillouin zone, and a cation defect is introduced, when it is re-

We dedicate this work to professor Woon-Sun Ahn on the occasion of this retirement.

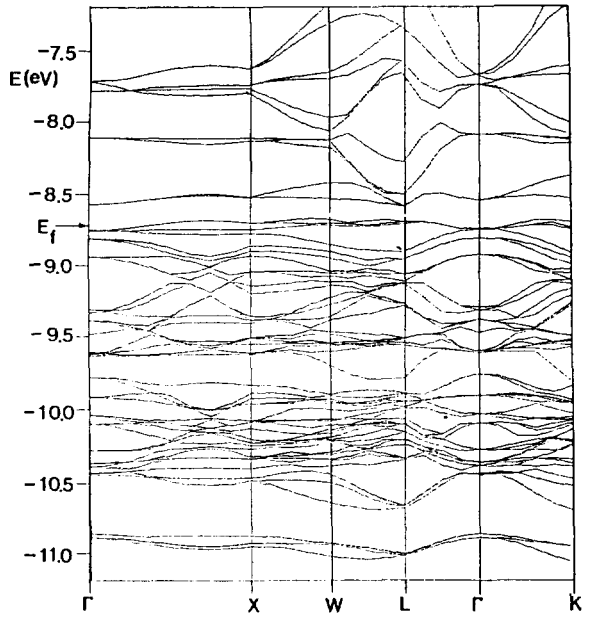

Figure 2. Total d-band structure of the cation defected NiO unit cell along the symmetry direction, Γ→X→W→L→Γ→K.

quired, by removing the nickel atom at the center of the octahedron formed by oxygen atoms. The band structure of the defected nickel oxide is calculated along the several symmetry directions of the Brillouin zone,[22] and the results are shown in Figure 2 and 3. The parameters and the lattice constants used in this calculation are given in the appendix at the end of this paper.

The band structures of Figure 2 shows the Fermi energy level E_f at −8.74 eV and d-band width of 4.4 eV. The calculated value of the d-band width agrees well with the value 4.3 eV, which is calculated using localized orbitals obtained in a self-consistent manner by Hugel *et al.*[3] Also, it is shown that the d-band structure near the Fermi level along the symmetry direction, Γ→*X* with a Ni defect at the octahedral center in Figure 3(a) and at the edge in Figure 3(b). The band gap between the valence and the conduction bands of the defected NiO calculated is about 0.2 eV near the Γ in contrast to the perfect NiO (in private calculation), showing that it behaves as a semiconductor in agreement with the experimental observation.[8,23] However, in most of the symmetry directions the band gap are close to Fermi level to be a metal or semimetal. Also, when the edge Ni atom (surface atom) is defected, the band gap is too narrow to be a semiconductor except near the Γ direction, presumably due to the edge effect in Figure 3(b). It has been known that the delocalized energy-band formalism such as EHT type fail to properly describe the electron structure of transition metal oxides.[19]

Electronic structure of the oxygen atom. A model consisting of two NiO unit cells is taken as shown in Figure 4 in order to find the effect of cation vacancy on the oxygen atom. The properties of oxygen atom at the octahedral center is then investigated with the cation defect placed on the octahedral surface number 1 and 2, corresponding to the surface (top and bottom plane) and inside lattice sites (body centered) of the nickel oxide, respectively. The properties are investigated by calculating the DOS, the COOP, the electron density, and the O 1s electron binding energy shift. The charges of the oxygen and nickel atoms adjacent to the defect site calculated are shown in Table 1.

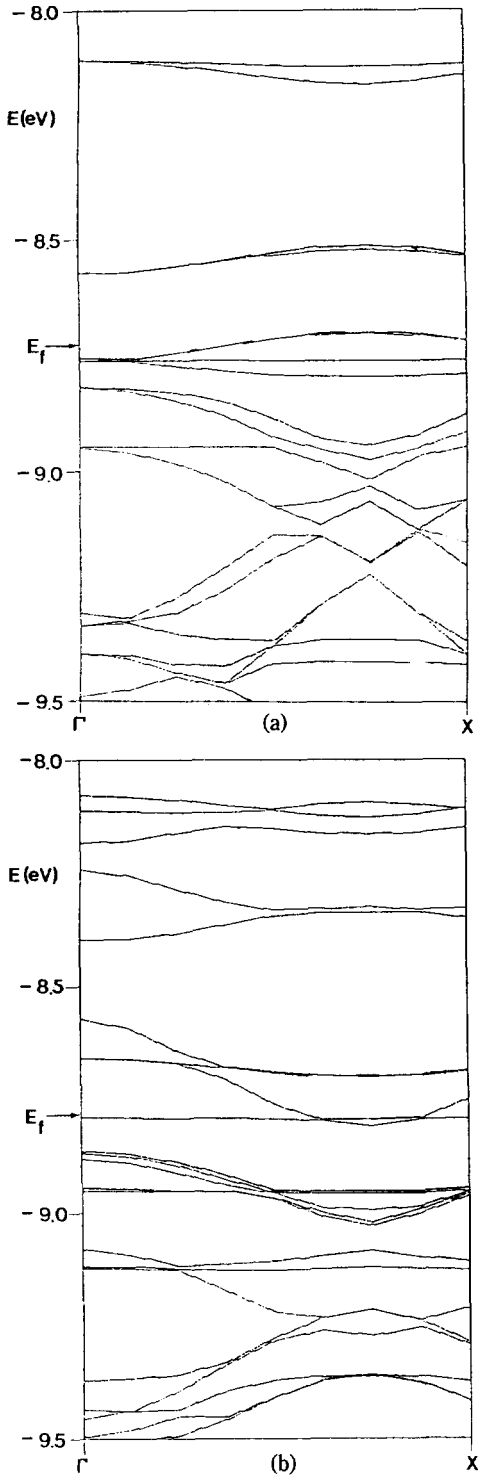

Figure 3. The d-band structure near the Fermi level along the symmetry direction, Γ→X with the Ni defect (a) at the octahedral center, and (b) at the edge.

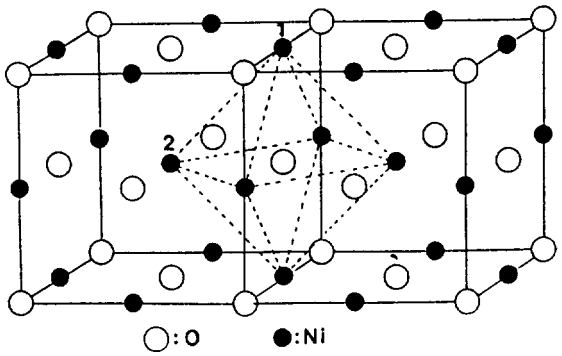

Figure 4. A model consisting of two NiO unit cells. Nickel atom numbered 1 corresponds to the surface atom, and the one numbered 2 the inner atom of the oxide.

Table 1. The average changes of net charge on the central oxygen atom and the adjacent nickel atoms due to a Ni defect

	Change of net charge	
	Centered oxygen	The nearest neighbor nickel
P	0.000	0.000
ID	−0.040	+0.264
SD	−0.075	+0.258

P: Perfect NiO structure, SD: Surface Ni atom (no. 1) is defected. ID: Inner Ni atom (no. 2) is defected. The following tables are the same notation.

In this work, the cation defect site considered is limited to the octahedral nickel positions only, and their effects on the central oxygen atom and the adjacent nickel atoms are considered exclusively. According to the Table 1, the defect decreases in general the net charge on the oxygen atom while it increases the net charge on the adjacent nickel atoms. These net charge decrease of the oxygen atom, which corresponds to the decrease of its oxidation degree, will deshielded the nuclear to the core electrons to increase their binding energies. The changes of electron densities in the various orbitals of the oxygen atom and the adjacent nickel atoms are calculated in order to find the effects of the defect introduction at the level of electronic energy, and the results are shown in Table 2. The corresponding DOS of the oxygen p-orbitals and the nickel d-orbitals are shown in Figure 5 and 6.

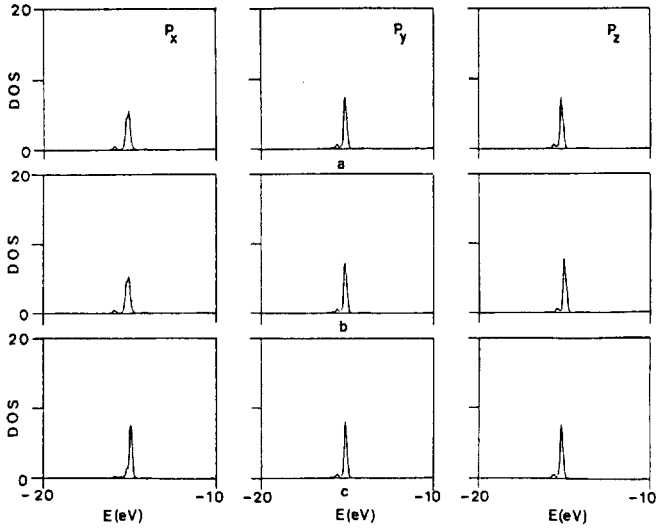

Figure 5. Projected DOS of the oxygen p-orbitals in (a) perfect, (b) surface nickel defected, and (c) inner nickel defected NiO models.

Table 2 shows that the surface Ni defect increases the electron density of the oxygen p_z-orbital, while the inner defect increases that of the oxygen p_x-orbital. The total electron density of the p-orbitals is increased more when the defect is on the surface rather than it is in the inside. It is clear that the defect gives a different degree of effect on the oxygen atom depending on its location. This means that oxygen atom can assume a few different oxidized states in the defected NiO. The identical effects can be seen in Figure 5. That is, the p_z-orbital DOS changes most significantly when the surface nickel atom is defected, while the change takes place in the p_x-orbital DOS significantly when one of the inner atom is defected.

Table 2. The changes of electron density of oxygen and the adjacent nickel atoms due to the Ni defect

	electron density change of oxygen atom				
	Δs	Δp_x	Δp_y	Δp_z	Δtotal
P	0.000	0.000	0.000	0.000	0.000
ID	0.003	0.071	−0.033	−0.002	0.039
SD	0.003	−0.002	−0.033	0.105	0.073

	electron density change of the nearest neighbor nickel									
	Δs	Δp_x	Δp_y	Δp_z	$\Delta d_{x^2-y^2}$	Δd_{z^2}	Δd_{xy}	Δd_{xz}	Δd_{yz}	Δtotal
P	0.000	0.000	0.000	0.000	0.000	0.000	0.000	0.000	0.000	0.000
ID	−0.012	0.008	−0.012	0.000	−0.390	−0.650	0.000	0.000	0.000	−1.056
SD	−0.008	0.004	−0.008	0.004	−0.334	−0.692	0.000	0.000	0.001	−1.038

Δ = defective structure − perfect structure.

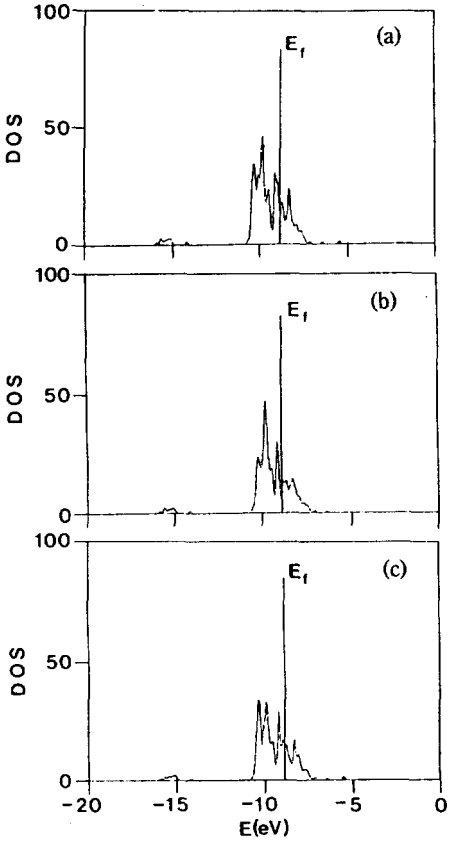

Figure 6. The total d-DOS of NiO in the states of (a) perfect, (b) surface nickel defected, and (c) inner nickel defected NiO models.

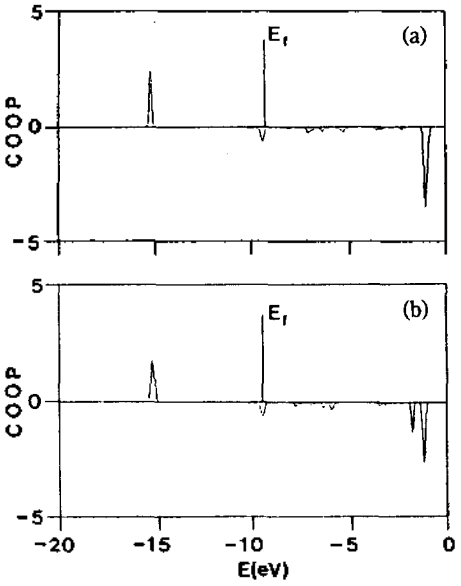

Figure 7. COOP of the Ni-Ni in (a) perfect, and (b) surface Ni defected NiO.

Table 2 shows at the same time that the defect causes the electron densities of the Ni e_g orbital ($d_{x^2-y^2}$, and d_{z^2}) to be decreased. This decrease of the electron density means, in turn, the increased oxidation state of the nickel

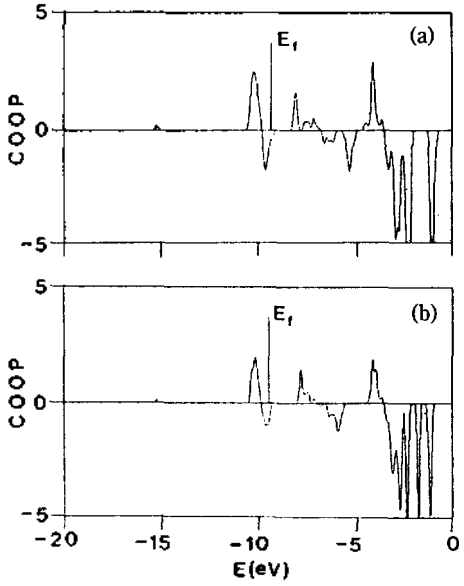

Figure 8. COOP of the Ni-O in (a) perfect, and (b) surface Ni defected NiO.

Table 3. The calculated valence potential of oxygen atom and the binding energy shift of 0 is electron due to the Ni defect (eV).

The theoretical				
Defect site		P	ID	SD
Valence potential		−197.5	−196.1	−195.3
Binding energy shift (ΔBE)		0.0	1.4	2.2
The experimental				
Oxygen atoms		I	II	III
Binding energy	(a)	529.7	531.4	
	(b)	529.6	531.0	531.4
Binding energy shift	(a)	0.0	1.7	
observed (ΔBE)	(b)	0.0	1.4	1.8

(a) ref. 13, (b) ref. 14. The theoretical and the experimental ΔBE are calculated in reference to the perfect structure of NiO(P) and to the oxygen atom(I), respectively.

atom. The change of the Ni d-DOS due to the defect shows also the decrease of electron density on the nickel atom. According to Figure 6, the Ni d-DOS below the fermi level decreases by the Ni defect, and this decrease means, in turn, a decrease of electrons in the d-orbital since the integral of the density of states below the fermi energy level multiplied by two gives the number of electrons.[24]

The COOP calculated shows that the nearest Ni-Ni bonding decreases while the nearest Ni-O bonding increases in the region below the fermi level when the surface Ni atom is defected. The inner Ni atom defect causes a less effect on the COOP.

Binding energy shifts of oxygen core electron. The O 1s binding energy shifts of a non-stoichiometric NiO are calculated with the valence potential model[25~29] by the EHT

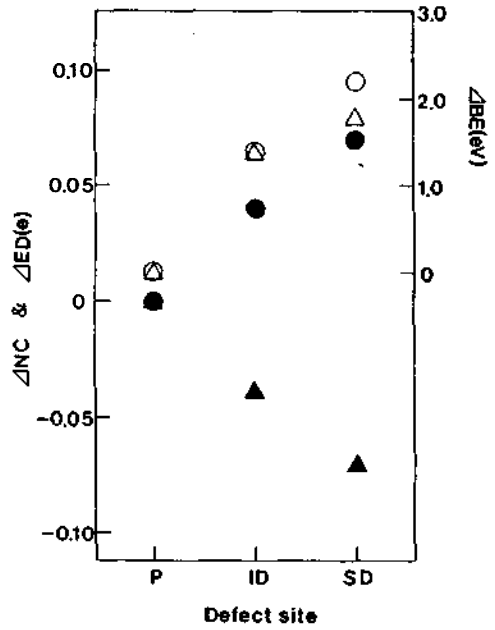

Figure 9. The change of net charge (ΔNC), electron density (ΔED) of oxygen atom, the shift of O 1s electron binding energy (ΔBE) due to defected Ni (P, SD and ID), and experimental ΔBE (I, II, III).[14]

method, and the results are given in Table 3.

As shown in Table 3, the valence potential of the oxygen atom is affected by the defect to different degrees depending on the defect site, and so is the core electron binding energy accordingly. The calculated shifts agree very well with those measured with photoelectron spectra of NiO.[13,14] It is now clear that the several O 1s peaks of the XPS of pure NiO are due to the defects. It is certain that the several oxidized states of oxygen atoms in NiO is inherent one due to the defects.

Finally, the core electron binding energy shift, the electron density change, and the net charge of oxygen atom are shown altogether in connection with the defect site (Figure 9). It can be seen that all of these properties are affected much more by the surface Ni defect than the inside one.

Acknowledgment. The present studies were supported by the Basic Science Research Institute program, Ministry of Education, 1994, project No. 3421.

Appendix. The calculation were made with the tight-binding EHT method using PC/386 and PC/486. The EH-MACC and EHPC of QCPE 571 (VAX version)[30] were converted into the MS-Fortran version and this program was complied by MS-Fortran version 5.0 under OS/2 version 1.1. The parameters used in this calculation are obtained by the charge iteration method due to Hoffmann.[31] The lattice constant used in this calculation is 4.1769 Å[23] and 26 K point set is used.

References

1. Heine, V.; Mattheiss, L. F. *J. Phys.* **1971**, *C4*, L191.
2. Kunz, A. B. *J. Phys.* **1981**, *C14*, L455.
3. Hugel, J.; Carabatos, C. *J. Phys.* **1983**, *C16*, 6713.
4. Mattheiss, L. F. *Phys. Rev.* **1972**, *B5*, 290.
5. Mattheiss, L. F. *Phys. Rev.* **1972**, *B5*, 306.
6. Oguchi, T.; Terakura, K.; Williams, A. R. *Phys. Rev.* **1983**, *B28*, 6443.
7. Terakura, K.; Oguchi, T.; Williams, A. R.; Kübler, J. *Phys. Rev.* **1984**, *B30*, 4734.
8. Cox, P. A. *The Electronic Structure and Chemistry of Solids*; Oxford Univ. Press: New York, 1986, p 214.
9. Larkins, F. P.; Fenshan, P. J.; Sanders, J. V. *Trans. Fara. Soc.* **1970**, *66*, 1748.
10. Larkins, F. P.; Fenshan, P. J. *Trans. Fara. Soc.* **1970**, *66*, 1755.
11. Surrat, G. T.; Kunz, A. B. *Phys. Rev.* **1979**, *B19*, 2352.
12. Mckay, J. M.; Henrich, V. E. *Phys. Rev.* **1985**, *B32*, 6764.
13. Tomellini, M. *J. Chem. Soc. Faraday Trans. 1*, **1988**, *84*, 3501.
14. Gonzàlez-Elipe, A. R.; Holgado, J. P.; Alvarez, R.; Munuera, G. *J. Phys. Chem.* **1992**, *96*, 3080.
15. Arnaud, Y. P. *Appl. Surf. Sci.* **1992**, *62*, 21.
16. Hoffmann, R.; Lipscomb, W. H. *J. Chem. Phys.* **1962**, *36*, 2179.
17. Hoffmann, R. *J. Chem. Phys.* **1963**, *39*, 1397.
18. Whangbo, M. H.; Hoffmann, R.; Woodward, R. B. *Proc. R. Soc. Lond* **1979**, *A366*, 23.
19. Boorse, R. S.; Alemany, P.; Burlitch, J. M.; Hoffmann, R. *Chem. Mater.* **1993**, *5*, 459.
20. Albright, T. A.; Burdett, J. K.; Whangbo, M. H. *Orbital Interaction in Chemistry*; Wiley: New York, 1985.
21. Canadell, E.; Whangbo, M. H. *Chem. Rev.* **1991**, *91*, 965.
22. Seitz, F.; Turnbull, D. *Solid State Physics*; Academic Press: New York, Vol. 1, 1955, p 35.
23. West, A. R. *Solid State Chemistry and Its Applications*; John Wiley & Sons: Singapore, 1989, p 519.
24. Hoffmann, R. *Solid and Surface, A Chemist's View of Bonding in Extended Structure*; VCH, New York, 1988, p 27.
25. Schwartz, M. E. *Chem. Phys. Lett.* **1970**, *6*, 631.
26. Schwartz, M. E. *Chem. Phys. Lett.* **1970**, *7*, 78.
27. Davis, D. W.; Shirley, D. A. *Chem. Phys. Lett.* **1972**, *15*, 185.
28. Ghosh, P. K. *Introduction to photoelectron spectroscopy*; John Wiley & Sons Inc., 1983, p 63.
29. Lee, K. S.; Koo, H. J.; Park, Y. C.; Ahn, W. S. *Bull. Kor. Chem. Soc.* **1994**, *15*(2), 139.
30. Whangbo, M. H.; Evain, M.; Hughbanks, T.; Kertesz, M.; Wijeyesekera, S.; Wilker, C.; Zheng, C.; Hoffmann, R. QCPE 571, *QCPE Bull.* **1989**, *9*, 61.
31. Saillard, J. Y.; Hoffmann, R. *J. Am. Chem. Soc.* **1984**, *106*, 2006.